Classical and Quantum Gravity

PAPER

Black resonators and geons in AdS_5

IOP Publishing Classical and Quantum Gravity

Class. Quantum Grav. 36 (2019) 125011 (23pp) https://doi.org/10.1088/1361-6382/ab1d76

Black resonators and geons in AdS_5

Takaaki Ishii[1,2] and **Keiju Murata**[3,4]

[1] Department of Physics, Kyoto University, Kyoto 606-8502, Japan
[2] Institute for Theoretical Physics, Utrecht University, 3584 CC Utrecht, The Netherlands
[3] Department of Physics, Osaka University, Toyonaka, Osaka 560-0043, Japan
[4] Department of Physics, College of Humanities and Sciences, Nihon University, Tokyo 156-8550, Japan

E-mail: ishiitk@gauge.scphys.kyoto-u.ac.jp and murata.keiju@nihon-u.ac.jp

Received 14 November 2018, revised 17 April 2019
Accepted for publication 29 April 2019
Published 29 May 2019

Abstract

We construct dynamical black hole solutions with a helical symmetry in AdS_5, called black resonators, as well as their horizonless limits, called geons. We introduce a cohomogeneity-1 metric describing a class of black resonators and geons whose isometry group is $R \times SU(2)$. This allows us to study them in a wide range of parameters. We obtain the phase diagram for the black resonators, geons, and Myers–Perry-AdS_5, where the black resonators emerge from the onset of a superradiant instability of the Myers–Perry-AdS_5 with equal angular momenta and are connected to the geons in the small horizon limit. The angular velocities of the black resonators always satisfy $\Omega > 1$ in units of the AdS radius. A black resonator is shown to have higher entropy than a Myers–Perry-AdS_5 black hole with the same asymptotic charges. This implies that the Myers–Perry-AdS_5 can dynamically evolve into the black resonator under the exact $SU(2)$-symmetry although its endpoint will be further unstable to $SU(2)$-violating perturbations.

Keywords: black holes, general relativity, AdS/CFT correspondence

(Some figures may appear in colour only in the online journal)

1. Introduction

Black holes and their gravitational dynamics in asymptotically anti de Sitter (AdS) spacetime have been widely studied recently. Motivations for them partly come from the finding and development of the AdS/CFT duality [1–3]. It has been revealed that the gravity in asymptotically AdS spacetime and higher dimensions has rich aspects to be explored. (For instance, see [4] for a review of higher dimensional black holes.) To find black hole solutions is especially important for understanding the dynamics of the gravity in AdS. Here, we focus on rotating black holes. The higher dimensional generalization of the Kerr black hole solution, known as the Myers–Perry black hole [5], was generalized to include a cosmological constant in five dimensions [6] as well as in all dimensions [7, 8]. We will refer to a rotating black hole solution in higher dimensional AdS as Myers–Perry-AdS (MPAdS). The thermodynamics of MPAdS was carefully discussed in [9] (see also [10]), and phase transitions for the rotating black hole solutions were studied in [11].

Superradiance is a characteristic phenomenon of rotating black holes: A wave scattered by a rotating black hole gains a larger amplitude than the injected wave under a certain condition. By the superradiance, energy and angular momenta can be extracted from the rotating black hole, and it makes the gravitational dynamics of the rotating black holes complicated.

In AdS, the superradiance leads to a dramatic scenario of gravitational dynamics known as the superradiant instability [12, 13]. Asymptotically AdS spacetime has a timelike boundary at conformal infinity, where waves are reflected. Hence, for a rotating black hole in AdS, the wave amplified by the superradiance is injected back to the black hole. By repetitions of the process, the initial perturbation grows exponentially. In the Kerr-AdS_4 spacetime, a gravitational superradiant instability has been found in [14]. In the MPAdS spacetime, it has been found in [15–18] (see [19] for a review).

Once a superradiant instability occurs, new black hole solutions nonlinearly extending the instability are expected to appear. At the onset of a superradiant instability, there is a normal mode. In [15], it was conjectured that there is a family of black hole solutions branching from the MPAdS as the nonlinear extension of the normal mode. Such solutions have been numerically constructed in AdS_4 in [20] and named *black resonators*. These black holes are time periodic and have only a single helical Killing vector.

The first black resonators obtained in AdS_4 [20] are found by solving three-dimensional partial differential equations (PDEs) and are cohomogeneity-3 (i.e. the metric nontrivially depends on three coordinate variables). As far as they were studied (see also [21]), the angular velocities of the black resonators always satisfy $\Omega > 1$ in units of the AdS radius. In [22], it was shown that the AdS black holes with $\Omega > 1$ are always unstable. Therefore, the black resonators will have unstable modes. However, their detailed analysis has not been done because of the difficulty due to few symmetries. Hence, it would be desirable if there is a setup where the black resonators can be studied extensively.

In the zero-size limit of the black hole horizon, the superradiant frequencies reduce to normal modes in AdS. Geons are then obtained as the nonlinear extension of the AdS normal modes. They were constructed in asymptotically AdS spacetime both perturbatively and non-perturbatively [23–26].

In this paper, we construct a class of black resonators and geons which can be described by a cohomogeneity-1 metric in pure Einstein gravity in AdS_5. We consider the five-dimensional MPAdS ($MPAdS_5$) with equal angular momenta as the 'background' from which the black resonators appear. This background spacetime has an $R \times U(2)$ isometry group. We focus on the superradiant instability which preserves the $SU(2)$-symmetry of the $MPAdS_5$. The resulting spacetime maintains $R \times SU(2)$ symmetries, and we find that it is described by a cohomogeneity-1 metric. The Einstein equations hence reduce to ordinary differential equations (ODEs), and this allows us to study the black resonator and geon solutions in an extensive range of parameters.

The rest of this paper consists as follows. In section 2, we start from reviewing the five-dimensional $MPAdS_5$ solutions and superradiant instability relevant to this paper. In section 3, we introduce the metric ansatz for the cohomogeneity-1 black resonators and geons. In section 4, we construct the geons, first perturbatively and second fully numerically. In section 5, we obtain the black resonators and study their thermodynamics. We conclude in section 6 with a summary and discussions.

2. Superradiant instability of Myers–Perry-AdS$_5$ with equal angular momenta

In this section, we review the five-dimensional Myers–Perry-AdS black hole (MPAdS$_5$) with equal angular momenta and its superradiant instability. A black resonator is considered as the nonlinear extension of a rotating black hole's normal mode that exists at the onset of a superradiant instability. We will use the equal-angular-momentum MPAdS$_5$ as the 'background' to construct black resonators. For that purpose, we first summarize the black hole solution and its perturbations.

2.1. Myers–Perry-AdS$_5$ with equal angular momenta

We consider the pure Einstein gravity in five dimensions with a negative cosmological constant,

$$S = \frac{1}{16\pi G_5} \int d^5x \sqrt{-g} \left[R + \frac{12}{L^2} \right], \tag{2.1}$$

where G_5 is the five-dimensional Newton's constant, L is the AdS radius, and the cosmological constant is $\Lambda = -6/L^2$. Hereafter, we use units where $L = 1$. The Einstein equation is given by $G_{\mu\nu} - 6g_{\mu\nu} = 0$.

While in general the MPAdS$_5$ has two angular momenta J_1 and J_2, in the case of equal angular momenta $J_1 = J_2$, the metric of the MPAdS$_5$ can be given in a cohomogeneity-1 form [7][5],

$$ds^2 = -(1+r^2)f(r)d\tau^2 + \frac{dr^2}{(1+r^2)g(r)} + \frac{r^2}{4}\left[\sigma_1^2 + \sigma_2^2 + \beta(r)(\sigma_3 + 2h(r)d\tau)^2\right], \tag{2.2}$$

where the metric components are given by

$$g(r) = 1 - \frac{2\mu(1-a^2)}{r^2(1+r^2)} + \frac{2a^2\mu}{r^4(1+r^2)}, \quad \beta(r) = 1 + \frac{2a^2\mu}{r^4},$$
$$h(r) = \Omega - \frac{2\mu a}{r^4 + 2a^2\mu}, \quad f(r) = \frac{g(r)}{\beta(r)}. \tag{2.3}$$

The outer horizon of the black hole is located at $r = r_h$ that is the largest real root of $g(r_h) = 0$. The constant Ω may be shifted by a coordinate transformation. For later convenience, we choose Ω as follows so that $h(r_h) = 0$ is satisfied:

$$\Omega = \frac{2\mu a}{r_h^4 + 2a^2\mu}. \tag{2.4}$$

[5] These coordinates are brought to the Boyer–Lindquist coordinates in [7, 8] by $r^2 \to \frac{r^2+a^2}{1-a^2}$, $\theta \to 2\theta$, $\phi \to \varphi_1 - \varphi_2$, $\psi \to \varphi_1 + \varphi_2$, and $\mu \to \frac{M}{(1-a^2)^3}$ where ψ will be introduced later.

With this choice, we have $g_{\tau\tau}|_{r=r_h} = 0$. This implies that ∂_τ is the null generator of the horizon. In equation (2.2), we have introduced the one-forms σ_a $(a = 1, 2, 3)$ on S^3 as

$$\sigma_1 = -\sin\chi \mathrm{d}\theta + \cos\chi \sin\theta \mathrm{d}\phi,$$
$$\sigma_2 = \cos\chi \mathrm{d}\theta + \sin\chi \sin\theta \mathrm{d}\phi,$$
$$\sigma_3 = \mathrm{d}\chi + \cos\theta \mathrm{d}\phi \, . \tag{2.5}$$

We also find it convenient to define

$$\sigma_\pm = \frac{1}{2}(\sigma_1 \mp \mathrm{i}\sigma_2) = \frac{1}{2}\mathrm{e}^{\mp\mathrm{i}\chi}(\mp\mathrm{i}\mathrm{d}\theta + \sin\theta \mathrm{d}\phi) \, . \tag{2.6}$$

The one-forms satisfy the Maurer–Cartan equation $\mathrm{d}\sigma_a - 1/2\epsilon_{abc}\sigma_b \wedge \sigma_c = 0$. The angular coordinates ϕ and χ are defined on a twisted torus: the coordinate ranges are $0 \leqslant \theta \leqslant \pi$, $0 \leqslant \phi < 2\pi$, and $0 \leqslant \chi < 4\pi$ with the periodicity

$$(\theta, \phi, \chi) \sim (\theta, \phi + 2\pi, \chi + 2\pi) \sim (\theta, \phi, \chi + 4\pi) \, . \tag{2.7}$$

There are $SU(2)$ generators ξ_i $(i = x, y, z)$ defined by

$$\xi_x = \cos\phi \partial_\theta + \frac{\sin\phi}{\sin\theta}\partial_\chi - \cot\theta \sin\phi \partial_\phi,$$
$$\xi_y = -\sin\phi \partial_\theta + \frac{\cos\phi}{\sin\theta}\partial_\chi - \cot\theta \cos\phi \partial_\phi,$$
$$\xi_z = \partial_\phi, \tag{2.8}$$

which satisfy $[\xi_i, \xi_j] = \epsilon_{ijk}\xi_k$. The one-forms σ_a satisfy $\mathcal{L}_{\xi_i}\sigma_a = 0$ where $\mathcal{L}_{\xi_i}$ is the Lie derivative along the curve generated by the vector field ξ_i. Thus σ_a are invariant 1-forms of this $SU(2)$. We have $\sigma_1^2 + \sigma_2^2 = \mathrm{d}\theta^2 + \sin^2\theta \mathrm{d}\phi$, which gives the metric of a round S^2. Then, in equation (2.2), an $r =$ constant surface is given by a squashed S^3 written as a S^1 bundle over S^2.

There is another non-trivial Killing vector ∂_χ. This vector field generates a rotation of σ_1 and σ_2,

$$\mathcal{L}_{i\partial_\chi}\sigma_\pm = \pm\sigma_\pm, \quad \mathcal{L}_{i\partial_\chi}\sigma_3 = 0, \tag{2.9}$$

i.e. $\sigma_\pm$ and σ_3 have $U(1)$-charges ±1 and 0, respectively. The S^2 part of the metric, $\sigma_1^2 + \sigma_2^2 = 4\sigma_+\sigma_-$, is invariant under ∂_χ. Had there be no rotations, the round S^3 formed by $\sigma_{1,2,3}$ has had another $SU(2)$ symmetry which contains this ∂_χ, but in (2.2) it is broken down to $U(1)$ due to the angular momentum. In summary, the isometry group of the geometry (2.2) is given by $R_\tau \times SU(2) \times U(1) \simeq R_\tau \times U(2)$, where R_τ is the shift symmetry along the τ-direction.

The thermodynamics of MPAdS was discussed in [9, 10]. For the MPAdS$_5$ with equal angular momenta, the mass E, angular momentum J, entropy S, and temperature T are given by

$$E = \frac{\pi}{4G_5}\mu(a^2 + 3), \quad J = \frac{\pi}{G_5}\mu a,$$
$$S = \frac{\pi^2 r_h^3}{2G_5}\sqrt{1 + \frac{2\mu a^2}{r_h^4}}, \quad T = \frac{2(1 - a^2)r_h^4 + (1 - 4a^2)r_h^2 - 2a^2}{2\pi r_h^2\sqrt{(1 - a^2)r_h^2 - a^2}} \, . \tag{2.10}$$

The angular velocity Ω is given by equation (2.4).

2.2. Rotating and non-rotating frames at infinity

The solution given above actually corresponds to the *rotating frame* at infinity. The asymptotic form of the MPAdS$_5$ metric at the AdS boundary $r \to \infty$ becomes

$$ds^2 \simeq -(1+r^2)d\tau^2 + \frac{dr^2}{1+r^2} + \frac{r^2}{4}\left[\sigma_1^2 + \sigma_2^2 + (\sigma_3 + 2\Omega d\tau)^2\right] . \tag{2.11}$$

Meanwhile, we took $h(r_h) = 0$ on the horizon, and we deduce for the coordinate τ that ∂_τ becomes the null generator of the horizon.

We can move to the *non-rotating frame* at infinity by defining (t, ψ) as

$$dt = d\tau, \quad d\psi = d\chi + 2\Omega d\tau . \tag{2.12}$$

In these coordinates, the asymptotic form of the metric becomes

$$ds^2 \simeq -(1+r^2)dt^2 + \frac{dr^2}{1+r^2} + \frac{r^2}{4}\left[\bar{\sigma}_1^2 + \bar{\sigma}_2^2 + \bar{\sigma}_3^2\right] , \tag{2.13}$$

where we introduced the invariant one-forms for the non-rotating frame $\bar{\sigma}_a$ by replacing χ with ψ in equation (2.5): $\bar{\sigma}_1 = -\sin\psi d\theta + \cos\psi \sin\theta d\phi$, and so on. The explicit relation between σ_a and $\bar{\sigma}_a$ is

$$\sigma_\pm = e^{\pm 2i\Omega t}\bar{\sigma}_\pm, \quad \sigma_3 = \bar{\sigma}_3 - 2\Omega dt . \tag{2.14}$$

However, the combination $\sigma_1^2 + \sigma_2^2 = \bar{\sigma}_1^2 + \bar{\sigma}_2^2$ is invariant under the rotation. The null generator of the horizon is given by the linear combination of ∂_t and ∂_ψ as[6]

$$\frac{\partial}{\partial\tau} = \frac{\partial}{\partial t} + \Omega \frac{\partial}{\partial(\psi/2)} . \tag{2.15}$$

The trajectory of the horizon generator ∂_τ is rotating with the angular velocity Ω with respect to the non-rotating frame. This shows that equation (2.4) gives the angular velocity of the event horizon. In the rotating frame, we can view Ω as the boundary source of the rotation in the context of the AdS/CFT duality. In fact, Ω is identified as the rotation chemical potential.

2.3. Superradiant instability

Let us consider a linear perturbation of the MPAdS$_5$ with equal angular momenta. The gravitational superradiant instability of the MPAdS$_5$ has been found first in [16], and its detailed analysis also has been done in [18]. Here we focus on a τ-independent perturbation of the form[7]

$$\delta g_{\mu\nu}dx^\mu dx^\nu = \frac{r^2}{4}\delta\alpha(r)(\sigma_1^2 - \sigma_2^2) = \frac{r^2}{2}\delta\alpha(r)(\sigma_+^2 + \sigma_-^2) . \tag{2.16}$$

This perturbation is $SU(2)$-invariant, but the first and second terms in the last expression have the $U(1)$-charges $+2$ and -2, respectively. Other components of $SU(2)$-invariant perturbations cannot have $U(1)$-charges ± 2. (For example, dt^2 and $dt\sigma_+$ have the $U(1)$-charges 0

[6] We define the angular velocity Ω with respect to $\psi/2 \in [0, 2\pi)$ instead of ψ itself. This Ω matches the definition in other literature [9, 15, 16].

[7] We would like to point out that this perturbation actually corresponds to charged tensor harmonics on $CP^1 \simeq S^2$. It has been widely believed that there are no charged tensor harmonics on CP^1 because the transverse traceless conditions and eigenvalue equation appear to overconstrain the charged tensor harmonics. In appendix A, we show that those conditions are not independent and then explicitly construct the charged tensor harmonics on CP^1. We are grateful to Prof Harvey Reall for private communication.

and $+1$, respectively. Only $\sigma_\pm^2$ can have the charges ±2.) As a result, we obtain a decoupled perturbation equation for $\delta\alpha$,

$$\delta\alpha'' + \left(\frac{g'}{g} + \frac{3+5r^2}{r(1+r^2)}\right)\delta\alpha' + \frac{8}{(1+r^2)g}\left(\frac{\beta-2}{r^2\beta} + \frac{2\beta h^2}{(1+r^2)g}\right)\delta\alpha = 0\,. \tag{2.17}$$

The perturbation in the rotating frame (2.16) is τ-independent, but its expression is explicitly time periodic in the non-rotating frame:

$$\delta g_{\mu\nu}\mathrm{d}x^\mu \mathrm{d}x^\nu = r^2\delta\alpha(r)(\mathrm{e}^{4\mathrm{i}\Omega t}\bar{\sigma}_+^2 + \mathrm{e}^{-4\mathrm{i}\Omega t}\bar{\sigma}_-^2)/2. \tag{2.18}$$

This is a normal mode whose frequency is given by $\omega = \pm4\Omega$. This corresponds to the onset of a '$(J,M,K) = (0,0,\pm2)$' superradiant instability [16].

We numerically search the critical values of Ω when the equation (2.17) is solved by a nontrivial $\delta\alpha$ with trivial boundary conditions $\delta\alpha(r_h) = \delta\alpha(\infty) = 0$. We can find not only the fundamental normal mode but also its overtones, and we label the modes by $n = 0, 1, 2, \cdots$. In figure 1, we plot the angular velocities at the onset of the instabilities for $n \leqslant 3$ modes. The extreme MPAdS$_5$ saturates $\Omega_{\mathrm{ext}} = \sqrt{1 + 1/(2r_h^2)}$, and in the upper right region there are no black holes described by equation (2.2). All curves of the instability frequencies approach the extreme black hole frequency as r_h increases. The higher overtones with $n > 3$, which are not shown in the figure, also approach the extremal frequency quickly. The results for the $n = 0$ mode coincide with [16].

3. Cohomogeneity-1 geons and black resonators

In this section, generalizing equation (2.2), we introduce a metric ansatz for cohomogeneity-1 geons and black resonators in the five-dimensional asymptotically AdS spacetime. We discuss the symmetries that the ansatz possesses and argue that the ansatz is designed for the spacetime with a helical Killing vector field. We also derive the expressions for thermodynamic quantities.

3.1. Metric ansatz

In section 2.3, we found that there is a superradiant instability for the $SU(2)$-invariant perturbation (2.16). Here we consider the nonlinear extension of the normal mode from the onset of the $SU(2)$-invariant instability. As a nonlinear generalization of equation (2.16), we take the metric ansatz as

$$\begin{aligned}\mathrm{d}s^2 = -(1+r^2)f(r)\mathrm{d}\tau^2 + &\frac{\mathrm{d}r^2}{(1+r^2)g(r)}\\ &+ \frac{r^2}{4}\left[\alpha(r)\sigma_1^2 + \frac{1}{\alpha(r)}\sigma_2^2 + \beta(r)(\sigma_3 + 2h(r)\mathrm{d}\tau)^2\right]\,.\end{aligned} \tag{3.1}$$

This spacetime is still cohomogeneity-1: the metric nontrivially depends only on the radial coordinate r. We introduce a new function $\alpha(r)$ which deforms the S^2 base space. The product of the coefficients of σ_1^2 and σ_2^2 are fixed by the redefinition of the radial coordinate r. The $U(1)$-symmetry that exists in the MPAdS$_5$ with equal angular momenta is broken in this ansatz unless $\alpha(r)$ is identically one. It follows that the metric (3.1) only has the $R_\tau \times SU(2)$

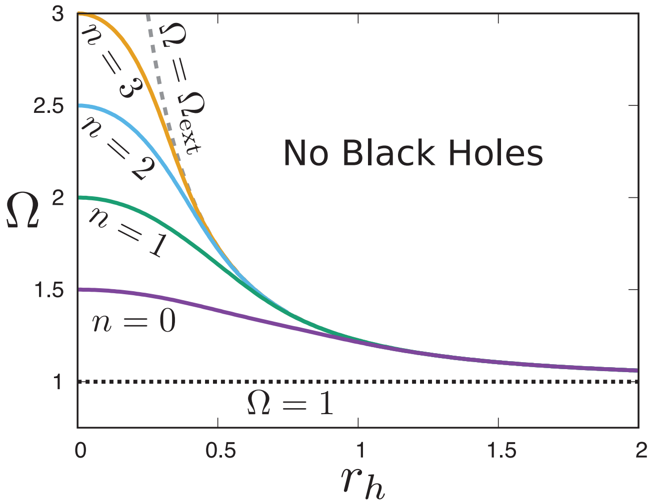

Figure 1. Onset of the superradiant instability of $MPAdS_5$. The frequency of the extreme $MPAdS_5$ $\Omega = \Omega_{\rm ext}$ is shown in a dashed line; there are no regular $MPAdS_5$ in the upper right region. We also plot $\Omega = 1$ in a dotted line which $\Omega_{\rm ext}$ asymptotes to in $r_h \to \infty$.

symmetries. If we set $\alpha(r) = 1$ trivially, our metric ansatz reduces to that for a $MPAdS_5$ black hole with equal angular momenta (2.2).

How does the metric (3.1) describe the black resonator and geon? Let us consider asymptotically AdS spacetime:

$$f(r) \to 1, \quad \alpha(r) \to 1, \quad \beta(r) \to 1 \quad (r \to \infty) \,. \tag{3.2}$$

Then $g(r) \to 1$ is automatically satisfied because of the Einstein equation. Meanwhile, the above condition does not restrict the asymptotic value of $h(r)$. We denote it by $\Omega \equiv h(\infty)$. Under the asymptotically AdS condition (3.2), the metric near the infinity becomes the same form as equation (2.11). The ansatz (3.1) indeed corresponds to the rotating frame: later, we will check that ∂_τ is normal to the horizon (i.e. $h(r)$ is zero at the horizon), but here we assume this.

Changing coordinates by equation (2.12), we can go to the non-rotating frame. However, we cannot simply shift the value of $h(\infty)$ while keeping the form of the metric (3.1). In the non-rotating frame, actually, there appears explicit periodic time dependence in the metric. This can be seen by rewriting the corresponding part of the metric with (t, ψ) as

$$\alpha\sigma_1^2 + \frac{1}{\alpha}\sigma_2^2 = 2\left(\alpha + \frac{1}{\alpha}\right)\bar{\sigma}_+\bar{\sigma}_- + \left(\alpha - \frac{1}{\alpha}\right)(\mathrm{e}^{4\mathrm{i}\Omega t}\bar{\sigma}_+^2 + \mathrm{e}^{-4\mathrm{i}\Omega t}\bar{\sigma}_-^2) \,. \tag{3.3}$$

The second part in the right hand side is a nonlinear generalization of equation (2.18).

As a consequence, the asymptotic time translation ∂_t and rotation ∂_ψ are *not* independently Killing vectors of the whole spacetime (3.1) unlike the $MPAdS_5$. Only an appropriate combination of ∂_t and ∂_ψ gives a Killing vector as follows:

$$K \equiv \frac{\partial}{\partial\tau} = \frac{\partial}{\partial t} + \Omega\,\frac{\partial}{\partial(\psi/2)} \,. \tag{3.4}$$

This Killing vector is 'helical' with respect to the asymptotically non-rotating frame (t, ψ). The asymptotic behavior of the norm of the Killing vector is

$$g_{\mu\nu}K^\mu K^\nu = g_{\tau\tau} \to -r^2(1-\Omega) \qquad (r \to \infty)\,. \tag{3.5}$$

For $\Omega > 1$, the Killing vector is asymptotically spacelike. Therefore, the solutions with $\Omega > 1$ and $\alpha(r) \neq 1$ express dynamical spacetime. In the following sections, we will construct such solutions. From equation (3.3), we find that the dynamical spacetime is time periodic with respect to the asymptotic time t. The solutions without a horizon are geons [24]. The solutions with horizons are called black resonators [20]. The cohomogeneity-1 metric (3.1) is a simple ansatz for studying geons and black resonators.

Because of the cohomogeneity-1 ansatz, the Einstein equations reduce to a set of ordinary differential equations:

$$\begin{aligned} f' =& \frac{1}{r(1+r^2)^2 g\alpha^2(r\beta'+6\beta)}[4r^2h^2(\alpha^2-1)^2\beta \\ &+ r(r^2+1)g\{r(1+r^2)f\alpha'^2\beta - r^3h'^2\alpha^2\beta^2 - 2(2+3r^2)f\alpha^2\beta'\} \\ &- 4(1+r^2)f\{6r^2\alpha^2\beta(g-1) + 3g\alpha^2\beta + (\alpha^2-\alpha\beta+1)^2 - 4\alpha^2\}], \end{aligned} \tag{3.6}$$

$$\begin{aligned} g' =& \frac{1}{6r(1+r^2)^2 f\alpha^2\beta}[-4r^2h^2(\alpha^2-1)^2\beta \\ &+ r(1+r^2)g\{-r(1+r^2)f\alpha'^2\beta + r^3h'^2\alpha^2\beta^2 \\ &- (-r(1+r^2)f' + 2f)\alpha^2\beta'\} + 4(1+r^2)f\{-6r^2\alpha^2\beta(g-1) - 3g\alpha^2\beta \\ &+ \alpha^4 + 4\alpha^3\beta - 5\alpha^2\beta^2 - 2\alpha^2 + 4\alpha\beta + 1\}], \end{aligned} \tag{3.7}$$

$$\begin{aligned} h'' =& \frac{1}{2r^2(1+r^2)\alpha^2\beta fg}[8fh(\alpha^2-1)^2 \\ &- r(1+r^2)h'\alpha^2\{r(fg'\beta - f'g\beta + 3fg\beta') + 10fg\beta\}], \end{aligned} \tag{3.8}$$

$$\begin{aligned} \alpha'' =& \frac{1}{2r^2(1+r^2)^2 f\alpha g\beta}[2r^2(r^2+1)^2fg\alpha'^2\beta \\ &- r(r^2+1)\alpha\alpha'\{r(1+r^2)(fg\beta)' + 2(3+5r^2)fg\beta\} \\ &- 8(\alpha^2-1)\{r^2h^2\beta(\alpha^2+1) - (1+r^2)f\alpha(\alpha-\beta) - (1+r^2)f\}], \end{aligned} \tag{3.9}$$

$$\begin{aligned} \beta'' =& \frac{1}{(2r^2(1+r^2))fg\alpha^2\beta}[-2r^4gh'^2\alpha^2\beta^3 \\ &- r\alpha^2\beta'\{r(1+r^2)(f'g\beta + fg'\beta - fg\beta') + 2(3+5r^2)fg\beta\} \\ &- 8f\beta(\alpha^4 + \alpha^3\beta - 2\alpha^2\beta^2 - 2\alpha^2 + \alpha\beta + 1)]\,. \end{aligned} \tag{3.10}$$

We will solve them numerically. In the case of four-dimensional AdS geons and black resonators, three-dimensional partial differential equations were solved [20, 24]. In contrast, considering five-dimensions and taking a special ansatz as in equation (3.1), we can reduce the problem to solving one-dimensional differential equations.

3.2. Boundary stress tensor and thermodynamic variables

The thermodynamic variables for our spacetime can be constructed from the data on the AdS boundary and horizon. Solving the equations of motion (3.6)–(3.10) near the AdS boundary, we obtain the asymptotic solution of the metric components as

$$f(r) = 1 + \frac{c_f}{r^4} + \cdots, \quad g(r) = 1 + \frac{c_f + c_\beta}{r^4} + \cdots,$$
$$h(r) = \Omega + \frac{c_h}{r^4} + \cdots, \quad \alpha(r) = 1 + \frac{c_\alpha}{r^4} + \cdots, \quad \beta(r) = 1 + \frac{c_\beta}{r^4} + \cdots, \tag{3.11}$$

where c_f, c_h, c_α, and c_β are the constants undetermined in the series solution.

We can employ the Ashtekar–Das method to construct conserved charges [27]. The stress energy tensor on the AdS boundary can be given by [28][8]

$$8\pi G_5 T_{ij} = -\frac{r^2}{2} C_{i\rho j\sigma} n^\rho n^\sigma \Big|_{r=\infty}, \tag{3.12}$$

where i, j run over the coordinates on the AdS boundary, n^μ is the unit normal to a bulk r-constant surface, and $C_{\mu\nu\rho\sigma}$ is the bulk Weyl tensor. Substituting the boundary expansion (3.11) into the above expression, we obtain

$$8\pi G_5 T_{ij} \mathrm{d}x^i \mathrm{d}x^j = \frac{1}{2}(c_\beta - 3c_f)\mathrm{d}\tau^2 + 2c_h \mathrm{d}\tau(\sigma_3 + 2\Omega \mathrm{d}\tau) - \frac{c_f + c_\beta}{8}(\sigma_1^2 + \sigma_2^2)$$
$$+ \frac{c_\alpha}{2}(\sigma_1^2 - \sigma_2^2) + \frac{1}{8}(-c_f + 3c_\beta)(\sigma_3 + 2\Omega \mathrm{d}\tau)^2 . \tag{3.13}$$

In the non-rotating frame (t, ψ), the boundary stress tensor is rewritten as

$$8\pi G_5 T_{ij} \mathrm{d}x^i \mathrm{d}x^j = \frac{1}{2}(c_\beta - 3c_f)\mathrm{d}t^2 + 2c_h \mathrm{d}t\bar{\sigma}_3 - \frac{c_f + c_\beta}{8}(\bar{\sigma}_1^2 + \bar{\sigma}_2^2)$$
$$+ c_\alpha(\mathrm{e}^{4\mathrm{i}\Omega t}\bar{\sigma}_+^2 + \mathrm{e}^{-4\mathrm{i}\Omega t}\bar{\sigma}_-^2) + \frac{1}{8}(-c_f + 3c_\beta)\bar{\sigma}_3^2 . \tag{3.14}$$

The energy density ($\propto T_{tt}$) and angular momentum density ($\propto T_{t\psi}$) depend on neither time nor spatial coordinates unlike the case of the four-dimensional geons and black resonators constructed in [20, 24]. Only the stress part (the coefficients of $\bar{\sigma}_\pm$) depends on the asymptotic time t. The energy and angular momentum are given by[9]

$$E = \int \mathrm{d}\Omega_3 T_{tt} = \frac{\pi(c_\beta - 3c_f)}{8G_5}, \quad J = -\int \mathrm{d}\Omega_3 T_{t(\psi/2)} = -\frac{\pi c_h}{2G_5} . \tag{3.15}$$

The entropy S and temperature T can be defined from the horizon data as

$$S = \frac{\pi^2 r_h^3 \sqrt{\beta(r_h)}}{2G_5}, \quad T = \frac{(1 + r_h^2)\sqrt{f'(r_h)g'(r_h)}}{4\pi} . \tag{3.16}$$

For these thermodynamic quantities, the first law of thermodynamics is

$$\mathrm{d}E = T\mathrm{d}S + \Omega \mathrm{d}J . \tag{3.17}$$

[8] This is equivalent to the holographic stress energy tensor derived by carrying out holographic renormalization [29, 30] up to the Casimir contribution which is absent in equation (3.12).
[9] We also define the angular momentum with respect to $\psi/2 \in [0, 2\pi)$.

In the case of the MPAdS$_5$, where we obtain equation (2.4) and equation (2.10), we can analytically check that this relation is satisfied [9][10]. In the numerical solutions of the geons and black resonators we will construct in the following sections, we check that the first law of thermodynamics is satisfied within numerical accuracy. For notational simplicity, we will set $G_5 = 1$ hereafter. We can easily recover the dependence on G_5 by $E \to G_5 E$, $J \to G_5 J$, and $S \to G_5 S$.

4. Geons

Geons appear nonlinearly from a normal mode of global AdS [23, 24]. For them, which are horizonless, the boundary condition at the center $r = 0$ of the global AdS is different from that for the black resonators. In this section, therefore, we treat the geons separately. We firstly consider the perturbative construction of the geons. We then compute full nonlinear solutions numerically.

4.1. Perturbative construction

Let us start from a linear perturbation of global AdS. The perturbation equation takes the same form as equation (2.17) where, as the background, we take the global AdS in a rotating frame at infinity: $f(r) = g(r) = \alpha(r) = \beta(r) = 1$ and $h(r) = \Omega$. Then, the perturbation equation can be solved analytically by

$$\delta\alpha = r^2(1+r^2)^{-2\Omega}{}_2F_1(1-2\Omega, 3-2\Omega; 4; -r^2)\,. \tag{4.1}$$

At the AdS boundary, this behaves

$$\delta\alpha \to \frac{6}{\Gamma(3-2\Omega)\Gamma(3+2\Omega)} \quad (r\to\infty)\,. \tag{4.2}$$

Therefore, $\delta\alpha$ satisfies $\delta\alpha \to 0$ in $r \to \infty$ only if $\Omega = (3+n)/2$ $(n = 0, 1, 2, \cdots)$. These corresponds to a tower of gravitational normal modes in the global AdS. The values at $r_h \to 0$ in figure 1 agree with these analytical results. Geons appear from these normal modes as nonlinear gravitational solutions.

We continue the perturbative expansion to higher orders and construct geons perturbatively in a way similar to [23–26]. (See appendix B for details.) Up to the fourth order in a small parameter ϵ, we obtain the perturbative expressions of E, J, and Ω for the geons as

$$\begin{aligned} &E = \frac{\pi}{8}\left(\frac{3}{10}\epsilon^2 + \frac{803}{84\,000}\epsilon^4\right), \quad J = \frac{\pi}{8}\left(\frac{1}{5}\epsilon^2 + \frac{2549}{378\,000}\epsilon^4\right), \\ &\Omega = \frac{3}{2} - \frac{1}{180}\epsilon^2 - \frac{356}{2338\,875}\epsilon^4\,. \end{aligned} \tag{4.3}$$

One can check that the first law of thermodynamics is satisfied: $\mathrm{d}E/\mathrm{d}J = (\mathrm{d}E/\mathrm{d}\epsilon)/(\mathrm{d}J/\mathrm{d}\epsilon) = \Omega + \mathcal{O}(\epsilon^4)$.

4.2. Numerical construction of the full geon solutions

To avoid a conical singularity at the center of the AdS $r = 0$, we impose a regular boundary condition there: $g(0) = 1$, $\alpha(0) = 1$ and $\beta(0) = 1$. Solving the equations of motion around $r = 0$, we obtain series solutions

[10] The normalization of our J is the same as that in [15], and it is related to the equal angular momentum case of $J_{a,b}$ in [9] as $J = J_a + J_b$ with $a = b$.

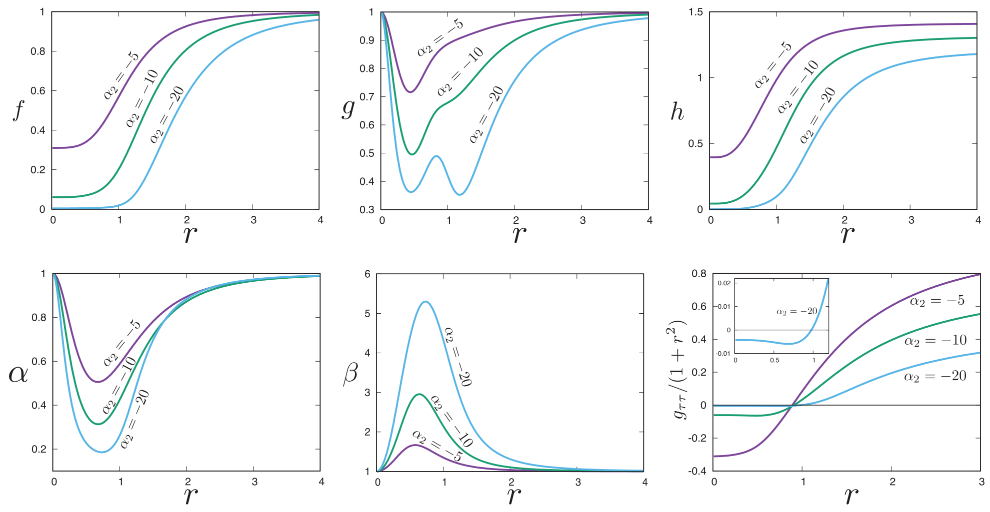

Figure 2. The metric components of the geons when $\alpha_2 = -5, -10, -20$. In the bottom-right, the norm of the Killing vector (3.4) is plotted.

$$f(r) = f_0 + \mathcal{O}(r^4), \quad g(r) = 1 - \beta_2 r^2 + \mathcal{O}(r^4), \quad h(r) = h_0 + \mathcal{O}(r^4),$$
$$\alpha(r) = 1 + \alpha_2 r^2 + \mathcal{O}(r^4), \quad \beta(r) = 1 + \beta_2 r^2 + \mathcal{O}(r^4)\,. \tag{4.4}$$

We have four free parameters, f_0, h_0, α_2, and β_2. When $\alpha_2 = 0$, the solution is simply the global AdS. To construct a geon solution, we turn on $\alpha_2 \neq 0$ as the parameter and tune the other three parameters f_0, h_0, and β_2 so that the asymptotically AdS conditions (3.2) are satisfied[11]. Without loss of generality, we can assume $\alpha_2 < 0$ because the field redefinition

$$\alpha(r) \to \frac{1}{\alpha(r)} \tag{4.5}$$

just exchanges the roles of σ_1 and σ_2. To find a solution, we use the Runge–Kutta method to integrate equations (3.6)–(3.10) and the Newton–Raphson method to determine the parameters f_0, h_0, and β_2. Numerical convergence is checked by changing resolutions.

In figure 2, the numerical geon solutions are shown for $\alpha_2 = -5, -10, -20$[12]. Their corresponding thermodynamical quantities are $(E, J, \Omega) = (2.11, 1.45, 1.41)$, $(5.84, 4.20, 1.31)$, $(15.3, 11.8, 1.21)$, respectively. The metric is clearly deformed from the pure AdS as $|\alpha_2|$ grows. In particular, the function $\alpha(r)$ measures the deformation of the base space S^2. We find a dip in the profile of $\alpha(r)$ around $r \simeq 0.8$. This indicates that the deformation of S^2 is localized around there. In the bottom-right panel of figure 2, we also show the norm of the Killing vector: $g_{\mu\nu}K^\mu K^\nu = g_{\tau\tau}$. For visibility, we normalize it by $1 + r^2$. Near the center of the AdS, K is timelike, i.e. the spacetime is stationary in this region. Far from the center ($r \gtrsim 1$), however, it becomes spacelike, and the spacetime is dynamical.

In figure 3, we plot the mass E and the angular velocity Ω as functions of the angular momentum J and compare them between the full numerical and perturbative solutions, which are shown

[11] We start from a normal mode for the global AdS, $f_0 = 1$, $h_0 = 3/2$, and $\beta_2 = 0$, and turn on a small α_2. Once we succeed in finding a solution, we vary α_2 slightly while using the previous result of (f_0, h_0, β_2) as an initial guess for a next solution.

[12] We consider the fundamental ($n = 0$) tone unless specified.

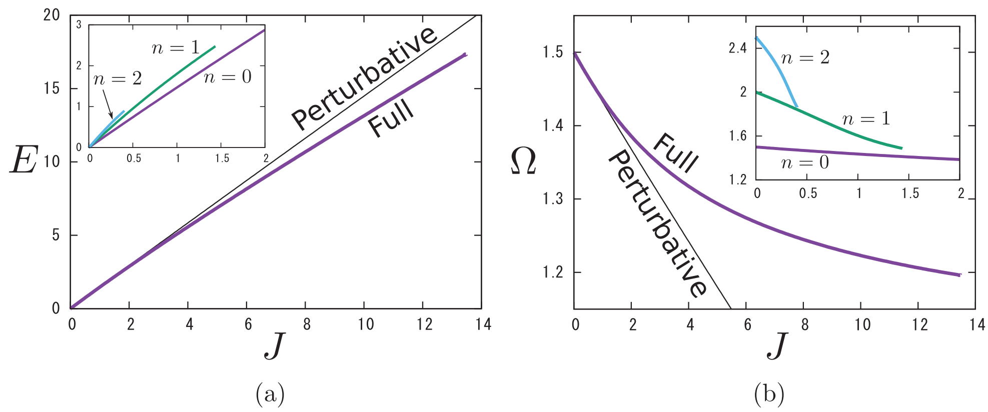

Figure 3. Mass E, angular momentum J and angular velocity Ω for the family of geons. E and Ω are shown as functions of J. Purple and black curves correspond to the numerically constructed full solutions and perturbative solutions, respectively. Those for overtones $n = 0, 1, 2$ are also shown in insets.

in the purple and black curves, respectively. For a small angular momentum $J \lesssim 1$, the perturbative results agree well with the numerical ones. In $J \gtrsim 1$, however, the former deviates clearly from the latter. We are able to obtain the geons even in a highly non-perturbative regime thanks to the cohomogeneity-1 metric ansatz (3.1). We also checked the first law of thermodynamics, $\mathrm{d}E/\mathrm{d}J = \Omega$, is satisfied within numerical accuracy. In the insets of the figure, we also plot E and Ω of the geons with the overtones $n = 0, 1, 2$ as functions of angular momentum J. The geons with higher overtones have larger energy. Although the curves for Ω are likely to intersect each other, we could not find the intersection within our numerical limitations.

5. Black resonators

In this section, we construct the black resonators numerically by solving the ordinary differential equations (3.6)–(3.10). We calculate the thermodynamic quantities for the black resonators and construct the phase diagram for the black holes. We also compare the thermodynamic quantities between the black resonators and MPAdS_5.

5.1. Numerical solutions

For black resonators, we impose that the metric functions $f(r)$ and $g(r)$ become zero at the horizon $r = r_h$. The asymptotic expansion near the horizon can be written in general as

$$\begin{aligned} &f(r) = f_1(r - r_h) + \cdots, \quad g(r) = g_1(r - r_h) + \cdots, \\ &h(r) = h_0 + h_1(r - r_h) + \cdots, \quad \alpha(r) = \alpha_0 + \alpha_1(r - r_h) + \cdots, \\ &\beta(r) = \beta_0 + \beta_1(r - r_h) + \cdots. \end{aligned} \tag{5.1}$$

Solving the equations of motion near the horizon, we find that $(f_1, h_1, \alpha_0, \beta_0)$ are not determined in the series expansion and the other coefficients are given in terms of them as

$$\begin{aligned} &g_1 = \frac{2(2r_h^2\alpha_0 + \alpha_0^2 - \alpha_0\beta_0 + 1)}{\alpha_0 r_h(1 + r_h^2)}, \quad \alpha_1 = \frac{2(\alpha_0^2 - 1)(\alpha_0^2 - \alpha_0\beta_0 + 1)}{r_h\beta_0(2r_h^2\alpha_0 + \alpha_0^2 - \alpha_0\beta_0 + 1)}, \\ &h_0 = 0, \quad \beta_1 = -\frac{r_h^2\beta_0^2 h_1^2}{f_1(1 + r_h^2)} - \frac{2(\alpha_0^4 + \alpha_0^3\beta_0 - 2\alpha_0^2\beta_0^2 - 2\alpha_0^2 + \alpha_0\beta_0 + 1)}{r_h\alpha_0(2r_h^2\alpha_0 + \alpha_0^2 - \alpha_0\beta_0 + 1)}. \end{aligned} \tag{5.2}$$

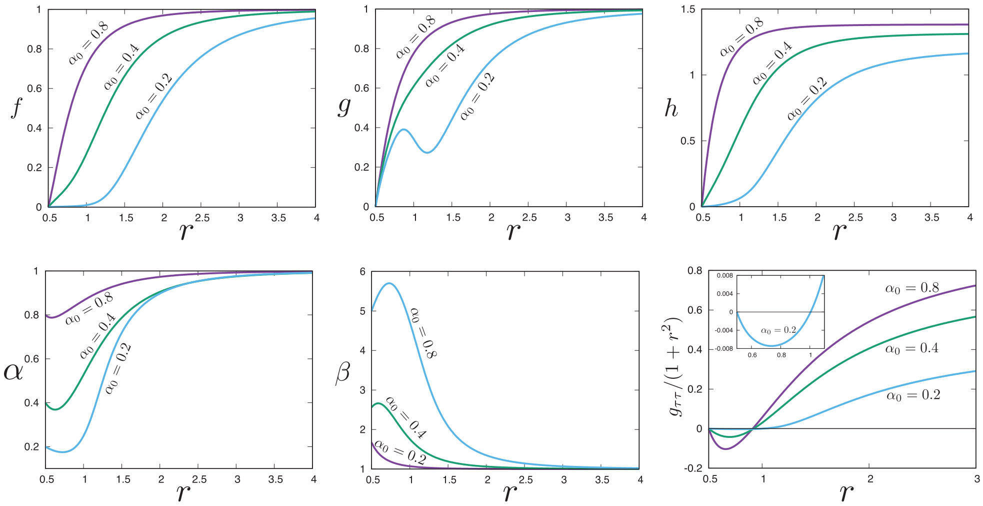

Figure 4. The metric components for the black resonators with $r_h = 0.5$ and $\alpha_0 = 0.8,\ 0.4,\ 0.2$. In the bottom-right panel, the norm of the Killing vector K is plotted.

As the lowest order equation in $r - r_h$, we obtain $(\alpha_0 - 1)h_0 = 0$. Both $\alpha_0 = 1$ and $h_0 = 0$ can solve this equation. The case of $\alpha_0 = 1$ corresponds to the MPAdS$_5$, where both $h_0 = 0$ and $h_0 \neq 0$ are allowed as we considered in section 2.2. If $\alpha_0 \neq 1$, we can construct the black resonator, but in this case we need $h_0 = 0$. We choose the latter here. Therefore, K is the null generator of the horizon in equation (3.1). There are five free parameters at the horizon: $(r_h, f_1, h_1, \alpha_0, \beta_0)$. Three of them can be fixed by matching them with the asymptotically AdS condition (3.2). Therefore, the black resonators are in a two parameter family. In our numerical calculations, we specify (r_h, α_0) as the parameters and tune (f_1, h_1, β_0) so that equation (3.2) is satisfied. For a given r_h, we start from a MPAdS solution at the onset of a superradiant instability and turn on a small deformation of α_0 from 1. Once a black resonator solution is successfully obtained, we use it as an initial guess for a next solution where α_0 is slightly varied. Without loss of generality, we assume $\alpha_0 < 1$ because of equation (4.5). We again use the Runge–Kutta and Newton–Raphson methods to obtain the black resonator solutions while assuring numerical convergence.

In figure 4, we show the metric components for the black resonator solutions with $r_h = 0.5$ and $\alpha_0 = 0.8,\ 0.4,\ 0.2$. Their corresponding thermodynamical quantities are $(E, J, \Omega, S, T) = (0.776, 0.337, 1.38, 0.798, 0.213)$, (3.95, 2.67, 1.32, 0.987, 0.111), (16.9, 13.0, 1.19, 1.38, 0.0203), respectively. We see that $\alpha(r)$ is deformed near the horizon and recovers the asymptotically AdS behavior as $r \to \infty$. Comparing figures 2 and 4, we find that the function profiles outside the horizon look similar, especially in $r \gtrsim 0.8$ in this case. This supports the notion that a black resonator is a dressed black hole where a black hole is placed inside a geon. In the bottom-right panel of figure 4, the norm of the Killing vector $g_{\mu\nu}K^\mu K^\nu$ is shown for the black resonators. Near the horizon, it is negative and the black resonator is stationary near the horizon. In a far region, the spacetime becomes dynamical. This property of the black resonator has been predicted in [15].

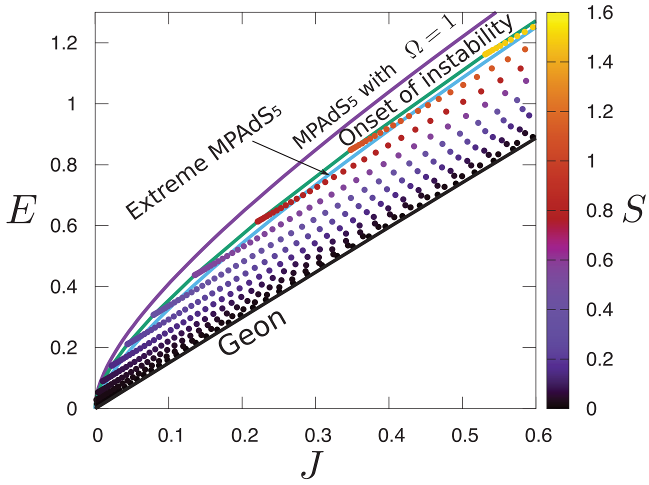

Figure 5. Phase diagram of the $MPAdS_5$ black holes, black resonators, and geons. The numerical data we constructed are marked with the dots in the (E, J) plane. The entropy S is shown by the color map. The black, purple, green, and light blue curves correspond to the geons, $MPAdS_5$ with $\Omega = 1$, $MPAdS_5$ at the onset of the superradiant instability, and extreme $MPAdS_5$, respectively.

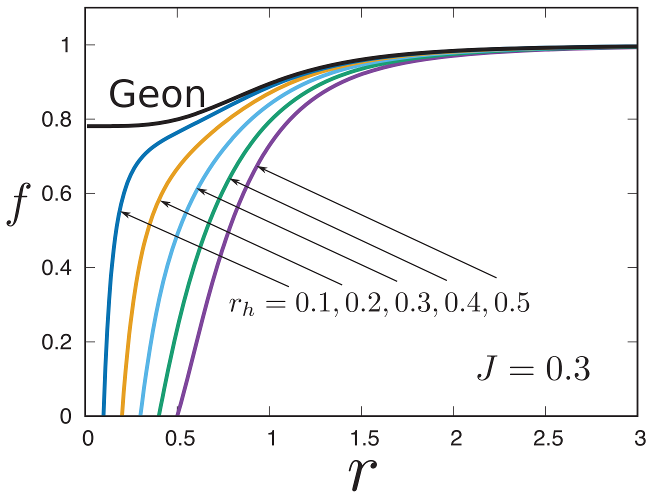

Figure 6. The metric component $f(r)$ for $r_h = 0.1, 0.2, \cdots, 0.5$. The angular momentum is fixed to $J = 0.3$.

5.2. Thermodynamics

Figure 5 shows the phase diagram of the $MPAdS_5$ black holes, black resonators, and geons on the (E, J) plane. The dots correspond to the data points that we numerically constructed. The black resonators branch from the onset of the superradiant instability of the $MPAdS_5$ black holes and can be found even in the region where no regular $MPAdS_5$ solutions exist. The black curve locating as the lower boundary is the family of the geons. The black resonators interpolate the onset of the instability of the $MPAdS_5$ black holes and the geons. The entropy of the black resonators is shown as a color map. It approaches zero near the geon limit. In figure 6,

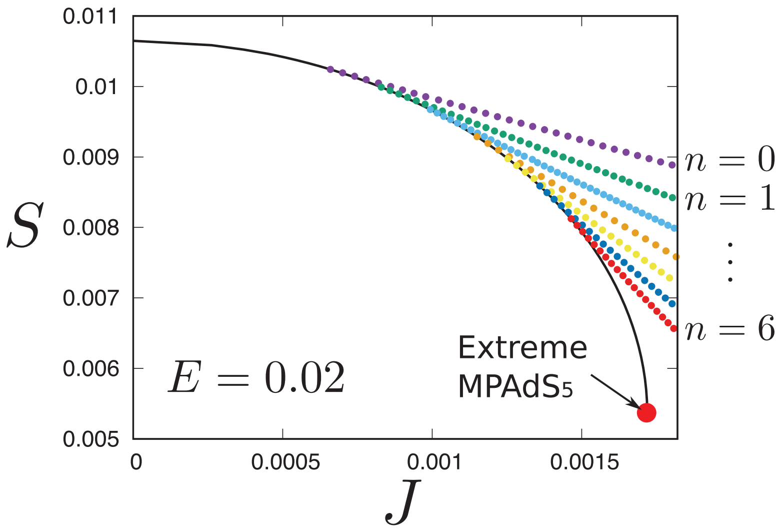

Figure 7. Comparison of S between the black resonators (dots) with $n = 0, 1, \cdots, 6$ and $MPAdS_5$ (black curve) for the same (E, J). The energy is fixed at $E = 0.02$ and the angular momentum is varied.

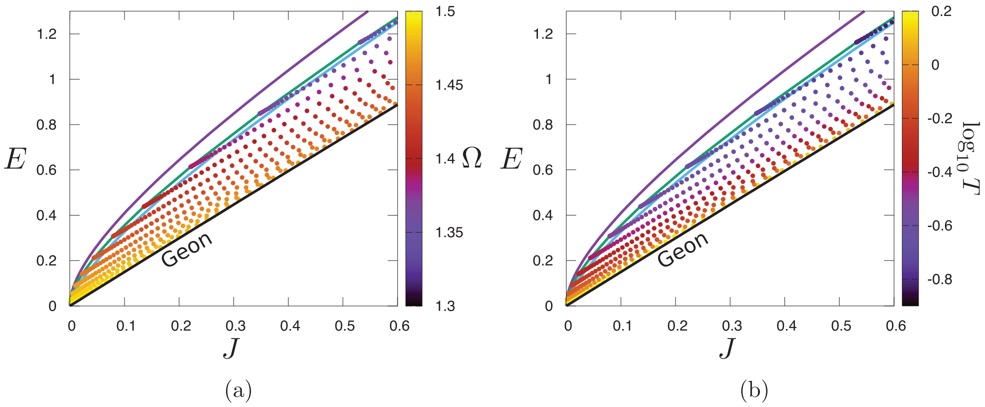

Figure 8. The angular velocity Ω and temperature T of the black resonators are shown as color maps on the (E, J) plane. (a) Angular velocity Ω. (b) Temperature T.

we compare the metric component $f(r)$ for the black resonators with different r_h at a fixed $J = 0.3$. This demonstrates that the functional profiles of the black resonators approach that of the geon as r_h decreases. For the numerical solutions, we monitored $\delta E - T\delta S - \Omega\delta J$ and found that this is consistent with zero within numerical accuracy.

The black resonators have larger entropy than the $MPAdS_5$ in the coexistence region as shown in figure 7. Families of black resonators branch from the $MPAdS_5$, and we plot data for the $n \leqslant 6$ tones. Extrapolated to arbitrary n, this result suggests infinite violation of uniqueness even for the black holes with the $R \times SU(2)$-symmetry. We find that the entropies of the black resonators are always larger than that of the $MPAdS_5$. Comparing the entropies of the black resonators between the data in the figure, we find that the fundamental tone ($n = 0$) has the largest entropy. This result indicates that, in dynamical processes, the $MPAdS_5$ causing the

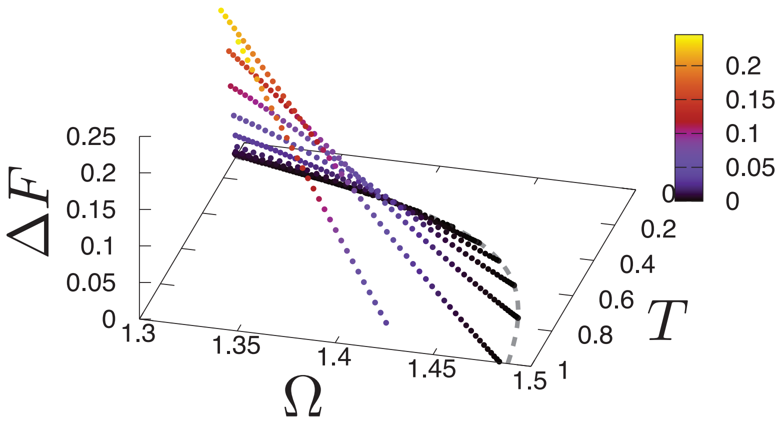

Figure 9. The difference of the free energy of the $n = 0$ black resonators from that of the MPAdS$_5$: $\Delta F \equiv F|_{\text{black resonator}} - F|_{\text{MPAdS}}$. We find $\Delta F > 0$ for $\alpha_0 \neq 1$. The onset of the superradiant instability, where $\Delta F = 0$, is also shown in a gray dashed curve.

superradiant instability can develop into the black resonators with $n = 0$ if the $SU(2)$-symmetry is imposed.

Figure 8 shows the angular velocity Ω and temperature T of the black resonators as color maps. The angular velocity is always greater than 1 and the horizon Killing vector becomes spacelike near the infinity $r = \infty$. This indicates that the black resonators found in this paper would suffer from further superradiant instabilities, probably to $SU(2)$-violating modes [21, 22]. In AdS$_4$, black resonators with $\Omega < 1$ cannot exist because of the rigidity theorem [31, 32]. In AdS$_5$, while the $U(1)$-symmetry generated by ∂_ψ is broken, ∂_ϕ can be still preserved. There may be a possibility of the existence of the black resonators with $\Omega < 1$, but so long as we studied, we did not find any in AdS$_5$. The temperature increases near the geons because the horizon radius is becoming small in the 'small black hole' branch.

In figure 9, we compare the free energy $F = E - TS - \Omega J$ between the MPAdS$_5$ and black resonators for the same (T, Ω). Thermodynamically, the free energy of the black resonators is higher than that of the MPAdS$_5$ black holes. Note that this comparison is in the small black hole region, and in any case both of these solutions have higher free energies than the thermal AdS, which would be the grand state.

6. Conclusions

We constructed the black resonators emerging from the onset of a superradiant instability of the MPAdS$_5$ with equal angular momenta. Geons were also obtained in their horizonless limit, which are nonlinear extensions of the normal modes of the global AdS. We used a cohomogeneity-1 metric ansatz for the black resonators and geons, which has a $SU(2)$ symmetry. It reduces the Einstein equations to ODEs and allows us to study the black resonators and geons in an extensive region in parameters. We demonstrated that the black resonators and geons have a helical Killing vector and are time periodic. We computed their thermodynamic quantities and obtained the phase diagram of the black resonators, geons, and MPAdS$_5$. The black resonators exist even in the region where no regular MPAdS$_5$ solutions do. They connect the onset of a superradiant instability of the MPAdS$_5$ and the geons. They have larger entropies than the MPAdS$_5$ in the coexistence region. We also constructed the black resonators with overtones and found that they have lower entropies than the fundamental tone. This indicates that, in dynamical processes, a $MPAdS_5$ can evolve into a black resonator with the fundamental tone if the $SU(2)$ symmetry is imposed. As far as we studied, the angular velocity of the black resonator always satisfies $\Omega > 1$.

What is the dual picture of the black resonator in the context of the AdS/CFT duality? As shown in equation (3.14), in the non-rotating frame, the boundary stress tensor is time-periodic. This means that the state dual to the black resonator breaks the time translation symmetry to a discrete one. This sounds analogous to a time crystal. However, there is a no-go theorem about realization of time crystals in the ground state [33]. We have found in figure 9 that the black resonators are not thermodynamically dominant. This situation is consistent with the no-go theorem.

A benefit of this work's approach is the easiness to handle the dynamics corresponding to the superradiance because of the cohomogeneity-1 metric. As shown in [22], the black resonators with $\Omega > 1$ are unstable, and those we constructed will also develop into other spacetimes[13]. What perturbations will the black resonators be unstable to? How strong is the instability? To answer such questions, it is necessary to work on stability analysis. For the black resonators in AdS_4 [20], the perturbation equations will still be 3-dimensional PDEs. For the cohomogeneity-1 black resonators found in this paper, these will reduce to ODEs, and this will help us to carry out stability analysis directly. If we find instabilities of the black resonators, these will suggest a new family of black hole solutions which have multi-frequencies [34].

Investigating nonlinear time evolution of the superradiant instability would be an important future direction. Dynamical processes involving superradiant instabilities have been recently considered in $(1+3)$-spacetime dimensions by numerical time evolution in [35]. If we impose the $SU(2)$-symmetry on dynamical spacetime as we have done in equation (3.1), we will just need to solve the time evolution of $(1+1)$-dimensional PDEs. With such a simplification, we will be able to partially answer the question about the final fate of the superradiant instability. In a similar way, we will be also able to study the weakly turbulent instability of AdS [36] in the pure gravity setup (2.1). The gravitational weakly turbulent instability without a rotation has been studied in [37]. (See also [23] for a perturbative study.) Recently, the generalization beyond preserving the spherical symmetry has also been considered [38–42]. It would be favorable to take into account the effect of rotations also from our perspective.

Acknowledgments

The authors would like to thank Akihiro Ishibashi, Masashi Kimura, Harvey Reall, Jorge Santos, Takahiro Tanaka, and Benson Way for useful discussions and comments. We also thank the Yukawa Institute for Theoretical Physics at Kyoto University. Discussions during the YITP workshop YITP-T-18-05 'Dynamics in Strong Gravity Universe' were useful to complete this work. The work of TI was supported in part by the Netherlands Organisation for Scientific Research (NWO) under the VIDI grant 680-47-518 and the Delta-Institute for Theoretical Physics (Δ-ITP), which is funded by the Dutch Ministry of Education, Culture and Science (OCW), and in part by JSPS KAKENHI Grant Number 18H01214. The work of KM was supported by JSPS KAKENHI Grant Number 15K17658 and in part by JSPS KAKENHI Grant No. JP17H06462.

[13] It was conjectured that their endpoint may not be described within classical gravity [21].

Appendix A. Charged tensor and vector harmonics on CP^1

In section 2.3, we introduced the metric perturbation (2.16) which has the $U(1)$-charges ± 2. In this appendix, we consider that perturbation from the viewpoint of the CP^1 base. In particular, we explicitly construct charged tensor harmonics on CP^1 and show that the perturbation with the $U(1)$-charges ± 2 corresponds to the lowest charged tensor modes[14].

The Fubini–Study metric and Kähler potential on CP^1 are given by

$$\hat{g}_{ij}\mathrm{d}x^i\mathrm{d}x^j = \frac{1}{4}(\mathrm{d}\theta^2 + \sin^2\theta\mathrm{d}\phi^2), \quad A = \frac{1}{2}\cos\theta\mathrm{d}\phi, \tag{A.1}$$

where $i, j = \theta, \phi$. The Kähler form is defined as $J = \mathrm{d}A$. The conditions for a tensorial function Y_{ij} on CP^1 to be charged tensor harmonics are

$$D^iY_{ij} = 0, \quad \hat{g}^{ij}Y_{ij} = 0, \tag{A.2}$$

and

$$(D^2 + \lambda_T)Y_{ij} = 0, \tag{A.3}$$

where $D_i = \hat{\nabla}_i - \mathrm{i}mA_i$ with $\hat{\nabla}$ being the covariant derivative with respect to $\hat{g}_{ij}$, and λ_T denotes the eigenvalue of $-D^2 = -D^iD_i$. Equation (A.2) corresponds to the transverse and traceless (TT) condition. The charge m corresponds to the eigenvalue of $-\mathrm{i}\partial_{\chi/2}$ ($\chi/2 \in [0, 2\pi)$) and must be an integer: $m \in \mathbf{Z}$[15].

A naive argument for non-existence of charged tensor harmonics could be given as follows. The number of the components of Y_{ij} is 3, and this equals the number of the TT condition (A.2). Therefore, Y_{ij} is completely determined just by the TT condition, and it would not further satisfy the eigenvalue equation (A.3). However, we will show that it actually does, and we will also explicitly obtain the charged tensor harmonics on CP^1.

Let us introduce the ansatz for the tensor harmonics as

$$Y_{ij} = \mathrm{e}^{\mathrm{i}n\phi}\begin{pmatrix} p(\theta) & q(\theta) \\ q(\theta) & -p(\theta)\sin^2\theta \end{pmatrix}. \tag{A.4}$$

Here, n is half-integer (integer) when m is odd (even) because of the periodicity (2.7). This trivially satisfies the traceless condition in equation (A.2). From the transverse condition, we obtain

$$\begin{aligned} &p'(\theta) + 2\cot\theta\, p(\theta) + \mathrm{i}\,\frac{2n - m\cos\theta}{2\sin^2\theta}\, q(\theta) = 0, \\ &q'(\theta) + 2\cot\theta\, q(\theta) - \frac{\mathrm{i}}{2}\,(2n - m\cos\theta)\, p(\theta) = 0\,. \end{aligned} \tag{A.5}$$

These can be analytically solved by

$$\begin{pmatrix} p(\theta) \\ q(\theta) \end{pmatrix} = c_1\begin{pmatrix} \mathrm{i}\ \cos^{a-2}(\theta/2)\ \sin^{b-2}(\theta/2) \\ 2\ \cos^{a-1}(\theta/2)\ \sin^{b-1}(\theta/2) \end{pmatrix} + c_2\begin{pmatrix} -\mathrm{i}\ \cos^{-a-2}(\theta/2)\ \sin^{-b-2}(\theta/2) \\ 2\ \cos^{-a-1}(\theta/2)\ \sin^{-b-1}(\theta/2) \end{pmatrix} \tag{A.6}$$

where $a = m/2 + n$ and $b = m/2 - n$. From the regularity at $\theta = 0$ and π, we find that a and b must be integers and satisfy

[14] The charged harmonics on CP^1 are also referred to as the monopole spherical harmonics. The scalar and vector monopole spherical harmonics are constructed in [43, 44]. See also [45] for an explanation that the monopole spherical harmonics are related to the spherical harmonics on S^3. Hence we expect that the perturbation (2.16) has its counterpart in the viewpoint of the base space.

[15] In the literature including [43], the charge $q = m/2$ is also used which takes the values in $q \in \mathbf{Z}/2$.

$$(a,b) \in \{a \geqslant 2, b \geqslant 2\} \quad \text{or} \quad (a,b) \in \{a \leqslant -2, b \leqslant -2\} . \tag{A.7}$$

For the former and later cases, we need to set $c_2 = 0$ and $c_1 = 0$, respectively. The condition equation (A.7) can be equivalently rewritten as

$$|m| = 2|n| + 4 + 2k \quad (k = 0, 1, 2, \cdots) . \tag{A.8}$$

In this way, we can completely determine Y_{ij} just from the TT conditions.

What is more, by a direct calculation, we can check that Y_{ij} also 'accidentally' satisfies the eigenvalue equation (A.3), and the eigenvalue is

$$\lambda_T = 2|m| - 8 . \tag{A.9}$$

Using equation (A.8), we find that the charged tensor harmonics on CP^1 exists only for $|m| \geqslant 4$. This is consistent with the fact that there is no uncharged tensor harmonics on CP^1. We can also explicitly check that

$$J^{ij} D_i Y_{jk} = 0 . \tag{A.10}$$

Therefore, all charged tensor harmonics on CP^1 are doubly transverse [15]. For $CP^{N\geqslant 2}$, there is an infinite infinite set of charged tensor harmonics for a fixed m [15]. Meanwhile, for CP^1, there are only finite numbers of the harmonics satisfying equation (A.8).

The gravitational perturbation (2.16) is then identified as a charged tensor perturbation on CP^1. We can write σ_-^2 in the components on S^2 as

$$(\sigma_-)_i(\sigma_-)_j = \frac{\mathrm{i}}{4} \mathrm{e}^{2\mathrm{i}\chi} \begin{pmatrix} \mathrm{i} & \sin\theta \\ \sin\theta & -\mathrm{i}\sin^2\theta \end{pmatrix} , \tag{A.11}$$

where the factor $\mathrm{e}^{2\mathrm{i}\chi}$ is for the S^1 fiber. This corresponds to the charged tensor harmonics with $m = 4$ and $n = 0$. Similarly, σ_+^2 corresponds to $m = -4$ and $n = 0$.

In a similar way, we can also explicitly construct the doubly transverse charged vector harmonics on CP^1. (Those on $CP^{N\geqslant 2}$ have been studied in [46].) As the solution of the doubly transverse conditions for a vectorial function Y_i, $D^i Y_i = J^{ij} D_i Y_j = 0$, we obtain

$$Y_i = c_1 \begin{pmatrix} \mathrm{i}\cos^{a-1}(\theta/2)\sin^{b-1}(\theta/2) \\ 2\cos^a(\theta/2)\sin^b(\theta/2) \end{pmatrix} + c_2 \begin{pmatrix} -\mathrm{i}\cos^{-a-1}(\theta/2)\sin^{-b-1}(\theta/2) \\ 2\cos^{-a}(\theta/2)\sin^{-b}(\theta/2) \end{pmatrix} . \tag{A.12}$$

From the regularity at $\theta = 0$ and π, we have

$$|m| = 2|n| + 2 + 2k \quad (k = 0, 1, 2, \cdots) . \tag{A.13}$$

This satisfies the eigenvalue equation $(D^2 + \lambda_V) Y_i = 0$ with

$$\lambda_V = 2|m| - 4 . \tag{A.14}$$

They exist only for $|m| \geqslant 2$.

Appendix B. Perturbative construction of the geons

In this appendix, we explain the construction of the perturbative geon results (4.3).

We consider a perturbative expansion of $\Phi(r) = (f(r), g(r), h(r), \alpha(r), \beta(r))^T$ as

$$\Phi(r) = \sum_{m=0}^{\infty} \Phi^{(m)}(r) \epsilon^m , \tag{B.1}$$

where ϵ is a small parameter. As the background, we take the global AdS_5 in the rotating frame: $\Phi^{(0)} = (1, 1, \Omega^{(0)}, 1, 1)^T$. In section 2.3, we showed that $\alpha^{(1)} = \delta\alpha$ satisfies the decoupled equation (2.17). It can be also easily checked that $f^{(1)} = g^{(1)} = h^{(1)} = \beta^{(1)} = 0$ in the leading order. The exact solution for $\alpha^{(1)}$ is given by equation (4.1). We focus on the fundamental tone: $\Omega^{(0)} = 3/2$. Then, we obtain

$$\alpha^{(1)}(r) = \frac{r^2}{(1+r^2)^3} \, . \tag{B.2}$$

We then go to the next order. The second order equations are written in the form

$$L\Phi^{(2)} = S^{(2)}, \tag{B.3}$$

where

$$L = \begin{pmatrix} L_{11} & L_{12} & 0 & 0 & L_{15} \\ 0 & L_{22} & 0 & 0 & L_{25} \\ 0 & 0 & L_{33} & 0 & 0 \\ 0 & 0 & 0 & L_{44} & 0 \\ 0 & 0 & 0 & 0 & L_{55} \end{pmatrix} \tag{B.4}$$

with

$$\begin{aligned} &L_{11} = \partial_r, \quad L_{12} = \frac{2(1+2r^2)}{r(1+r^2)}, \quad L_{15} = \frac{2+3r^2}{3(1+r^2)}\partial_r + \frac{2}{3r(1+r^2)}, \\ &L_{22} = \partial_r + \frac{2(1+2r^2)}{r(1+r^2)}, \quad L_{25} = \frac{1}{3(1+r^2)}\partial_r + \frac{10}{3r(1+r^2)}, \\ &L_{33} = \partial_r^2 + \frac{5}{r}\partial_r, \quad L_{44} = \partial_r^2 + \frac{3+5r^2}{r(1+r^2)}\partial_r - \frac{4(2-7r^2)}{r^2(1+r^2)^2}, \\ &L_{55} = \partial_r^2 + \frac{3+5r^2}{r(1+r^2)}\partial_r - \frac{8}{r^2(1+r^2)} \, . \end{aligned} \tag{B.5}$$

The source term $S^{(2)}$ is given by

$$\begin{aligned} S^{(2)} = &\bigg(-\frac{2r^3(1-4r^2)}{(1+r^2)^7}, \frac{2r^3(7-4r^2)}{(1+r^2)^7}, \frac{24r^2}{(1+r^2)^7}, \\ &\qquad \frac{2r^2(4-15r^2+8r^4)}{(1+r^2)^8}, -\frac{20r^2}{(1+r^2)^7} \bigg)^T . \end{aligned} \tag{B.6}$$

The second order equation (B.3) is solved by

$$\begin{aligned} \Phi^{(2)} = &\bigg(-\frac{3+18r^2+40r^4+20r^6+4r^8}{45(1+r^2)^6}, -\frac{r^2(30-25r^2+22r^4+5r^6)}{90(1+r^2)^6}, \\ &\quad \Omega^{(2)} - \frac{2+10r^2+5r^4+r^6}{20(1+r^2)^5}, \frac{r^4}{2(1+r^2)^6}, \frac{r^2(10+5r^2+r^4)}{30(1+r^2)^5} \bigg)^T, \end{aligned} \tag{B.7}$$

where $\Omega^{(2)}$ is an integration constant corresponding to the second order deviation of the angular velocity from the global AdS_5. This is actually determined from the third order analysis as we will see shortly. Other integration constants are determined by imposing the regularity at $r = 0$ and asymptotically AdS conditions (3.2).

The third order equation is given by

$$L\Phi^{(3)} = S^{(3)}, \tag{B.8}$$

where the α-component of $S^{(3)}$ is

$$S_\alpha^{(3)} = \frac{48\Omega^{(2)} r^2}{(1+r^2)^5} + \frac{2r^2(6 - 44r^2 + 637r^4 + 42r^6 - 17r^8 - 20r^{10})}{45(1+r^2)^{11}}, \tag{B.9}$$

and the other components are zero. Therefore, $f^{(3)} = g^{(3)} = h^{(3)} = \beta^{(3)} = 0$ are solutions to the third order. The equation of $\alpha^{(3)}$ can be analytically solved. From the asymptotically AdS condition $\alpha^{(3)} \to 0$ $(r \to \infty)$, the second order deviation of the angular velocity is determined as

$$\Omega^{(2)} = -\frac{1}{180}\,. \tag{B.10}$$

From equation (B.7), the asymptotic forms of the second order perturbations are given by

$$f^{(2)} = -\frac{4}{45r^4} + \cdots, \quad h^{(2)} = \Omega^{(2)} - \frac{1}{20r^4} + \cdots, \quad \beta^{(2)} = \frac{1}{30r^4} + \cdots\,. \tag{B.11}$$

The second order deviations of c_f, c_h and c_β, defined in equation (3.11), are hence $c_f^{(2)} = -4/45$, $c_h^{(2)} = -1/20$ and $c_\beta^{(2)} = 1/30$. Then, from equation (3.15), the second order contributions for the mass and angular momentum are obtained as

$$E^{(2)} = \frac{\pi}{8} \times \frac{3}{10}, \quad J^{(2)} = \frac{\pi}{8} \times \frac{1}{5}\,. \tag{B.12}$$

We can go to the higher orders by continuing the same procedure. As the fourth order equation, we have $L\Phi^{(4)} = S^{(4)}$ where all components of $S^{(4)}$ are non-zero. We can solve the equation analytically and find that $\Omega^{(4)}$, which is a constant term in $h^{(4)}$, is not determined from the boundary conditions in this order. However, at the fifth order, we obtain a decoupled equation for $\alpha^{(5)}$. Imposing $\alpha^{(5)} \to 0$ $(r \to \infty)$, we obtain

$$\Omega^{(4)} = -\frac{356}{2338\,875}\,. \tag{B.13}$$

From the asymptotic behaviour of the fourth-order perturbative solution with the above $\Omega^{(4)}$, we obtain the fourth-order deviation of the mass and angular momentum as

$$E^{(4)} = \frac{\pi}{8} \times \frac{803}{84\,000}, \quad J^{(4)} = \frac{\pi}{8} \times \frac{2549}{378\,000}\,. \tag{B.14}$$

Putting together the above results, we obtain equation (4.3).

ORCID iDs

Takaaki Ishii https://orcid.org/0000-0003-3034-4499
Keiju Murata https://orcid.org/0000-0001-9319-2993

References

[1] Maldacena J M 1999 The Large N limit of superconformal field theories and supergravity *Int. J. Theor. Phys.* **38** 1113–33
Maldacena J M 1998 *Adv. Theor. Math. Phys.* **2** 231
[2] Gubser S S, Klebanov I R and Polyakov A M 1998 Gauge theory correlators from noncritical string theory *Phys. Lett.* B **428** 105–14
[3] Witten E 1998 Anti-de Sitter space and holography *Adv. Theor. Math. Phys.* **2** 253–91
[4] Emparan R and Reall H S 2008 Black holes in higher dimensions *Living Rev. Relativ.* **11** 6
[5] Myers R C and Perry M J 1986 Black holes in higher dimensional space-times *Ann. Phys.* **172** 304
[6] Hawking S W, Hunter C J and Taylor M 1999 Rotation and the AdS / CFT correspondence *Phys. Rev.* D **59** 064005
[7] Gibbons G W, Lu H, Page D N and Pope C N 2005 The general Kerr–de Sitter metrics in all dimensions *J. Geom. Phys.* **53** 49–73
[8] Gibbons G W, Lu H, Page D N and Pope C N 2004 Rotating black holes in higher dimensions with a cosmological constant *Phys. Rev. Lett.* **93** 171102
[9] Gibbons G W, Perry M J and Pope C N 2005 The First law of thermodynamics for Kerr–anti-de Sitter black holes *Class. Quantum Grav.* **22** 1503–26
[10] Papadimitriou I and Skenderis K 2005 Thermodynamics of asymptotically locally AdS spacetimes *J. High Energy Phys.* JHEP08(2005)004
[11] Carter B M N and Neupane I P 2005 Thermodynamics and stability of higher dimensional rotating (Kerr) AdS black holes *Phys. Rev.* D **72** 043534
[12] Detweiler S L 1980 Klein–Gordon equation and rotating black holes *Phys. Rev.* D **22** 2323–6
[13] Cardoso V and Dias O J C 2004 Small Kerr–anti-de Sitter black holes are unstable *Phys. Rev.* D **70** 084011
[14] Cardoso V, Dias O J C and Yoshida S 2006 Classical instability of Kerr–AdS black holes and the issue of final state *Phys. Rev.* D **74** 044008
[15] Kunduri H K, Lucietti J and Reall H S 2006 Gravitational perturbations of higher dimensional rotating black holes: tensor perturbations *Phys. Rev.* D **74** 084021
[16] Murata K 2009 Instabilities of Kerr–AdS(5) × S∗∗5 Spacetime *Prog. Theor. Phys.* **121** 1099–124
[17] Kodama H, Konoplya R A and Zhidenko A 2009 Gravitational instability of simply rotating AdS black holes in higher dimensions *Phys. Rev.* D **79** 044003
[18] Cardoso V, Dias O J C, Hartnett G S, Lehner L and Santos J E 2014 Holographic thermalization, quasinormal modes and superradiance in Kerr–AdS *J. High Energy Phys.* JHEP04(2014)183
[19] Brito R, Cardoso V and Pani P 2015 Superradiance *Lect. Notes Phys.* **906** 1–237
[20] Dias O J C, Santos J E and Way B 2015 Black holes with a single Killing vector field: black resonators *J. High Energy Phys.* JHEP12(2015)171
[21] Niehoff B E, Santos J E and Way B 2016 Towards a violation of cosmic censorship *Class. Quantum Grav.* **33** 185012
[22] Green S R, Hollands S, Ishibashi A and Wald R M 2016 Superradiant instabilities of asymptotically anti-de Sitter black holes *Class. Quantum Grav.* **33** 125022
[23] Dias O J C, Horowitz G T and Santos J E 2012 Gravitational turbulent instability of anti-de Sitter space *Class. Quantum Grav.* **29** 194002
[24] Horowitz G T and Santos J E 2015 Geons and the instability of anti-de Sitter spacetime *Surv. Differ. Geom.* **20** 321–35
[25] Martinon G, Fodor G, Grandclment P and Forgcs P 2017 Gravitational geons in asymptotically anti-de Sitter spacetimes *Class. Quantum Grav.* **34** 125012
[26] Fodor G and Forgcs P 2017 Antide Sitter geon families *Phys. Rev.* D **96** 084027
[27] Ashtekar A and Das S 2000 Asymptotically anti-de Sitter space-times: conserved quantities *Class. Quantum Grav.* **17** L17–30
[28] Kinoshita S, Mukohyama S, Nakamura S and Oda K-Y 2009 A holographic dual of Bjorken flow *Prog. Theor. Phys.* **121** 121–64
[29] Balasubramanian V and Kraus P 1999 A stress tensor for anti-de Sitter gravity *Commun. Math. Phys.* **208** 413–28
[30] de Haro S, Solodukhin S N and Skenderis K 2001 Holographic reconstruction of space-time and renormalization in the AdS / CFT correspondence *Commun. Math. Phys.* **217** 595–622

[31] Hollands S, Ishibashi A and Wald R M 2007 A higher dimensional stationary rotating black hole must be axisymmetric *Commun. Math. Phys.* **271** 699–722
[32] Moncrief V and Isenberg J 2008 Symmetries of higher dimensional black holes *Class. Quantum Grav.* **25** 195015
[33] Watanabe H and Oshikawa M 2015 Absence of quantum time crystals *Phys. Rev. Lett.* **114** 251603
[34] Choptuik M, Santos J E and Way B 2018 Charting islands of stability with multioscillators in anti-de Sitter space *Phys. Rev. Lett.* **121** 021103
[35] Chesler P M and Lowe D A 2018 Nonlinear evolution of the AdS_4 black hole bomb (arXiv:1801.09711)
[36] Bizon P and Rostworowski A 2011 On weakly turbulent instability of anti-de Sitter space *Phys. Rev. Lett.* **107** 031102
[37] Bizon P and Rostworowski A 2017 Gravitational turbulent instability of AdS_5 *Acta Phys. Pol.* B **48** 1375
[38] Dias O J C and Santos J E 2016 AdS nonlinear instability: moving beyond spherical symmetry *Class. Quantum Grav.* **33** 23LT01
[39] Rostworowski A 2017 Higher order perturbations of antide Sitter space and time-periodic solutions of vacuum Einstein equations *Phys. Rev.* D **95** 124043
[40] Dias O J C and Santos J E 2018 AdS nonlinear instability: breaking spherical and axial symmetries *Class. Quantum Grav.* **35** 185006
[41] Bantilan H, Figueras P, Kunesch M and Romatschke P 2017 Nonspherically symmetric collapse in asymptotically AdS spacetimes *Phys. Rev. Lett.* **119** 191103
[42] Choptuik M W, Dias O J C, Santos J E and Way B 2017 Collapse and nonlinear instability of AdS space with angular momentum *Phys. Rev. Lett.* **119** 191104
[43] Wu T T and Yang C N 1976 Dirac monopole without strings: monopole harmonics *Nucl. Phys.* B **107** 365
[44] Weinberg E J 1994 Monopole vector spherical harmonics *Phys. Rev.* D **49** 1086–92
[45] Ishii T, Ishiki G, Shimasaki S and Tsuchiya A 2008 Fiber bundles and matrix models *Phys. Rev.* D **77** 126015
[46] Durkee M and Reall H S 2011 Perturbations of near-horizon geometries and instabilities of Myers-Perry black holes *Phys. Rev.* D **83** 104044